4.3. Ring closure reactions

Cyclization is an intramolecular reaction which takes place between the two ends of a cycle precursor and depends on the probability of their finding each other. It is in competition with an intermolecular reaction, which gives linear or cyclic oligomers. The intramolecular ring-closure is a first order reaction; its rate is proportional to the concentration of the cycle precursor. The intermolecular process is a second order reaction, however, and its rate is therefore proportional to the square of the concentration. Consequently, application of high dilution conditions should favour cyclization. Nevertheless there is no case known in which linear growth could be completely suppressed.

The number of building blocks used for a cyclization reaction is important because it determines the number of bond formation steps required on the way to the direct cycle precursor which is the compound that finally undergoes cyclization. The more such building blocks are involved, the less the overall synthetic effort is but there is a price to be paid for this which are low cyclization efficiency because of more side reactions and linear growth. Thus, the best strategy under the aspect of cyclization yields is to have a bisfunctional building block which is the macrocycle's direct precursor. However, this approach has the major disadvantage that this precursor's obtainment involves a time-consuming, multistep synthesis. Based on the present knowledge in this area it seems to be the best trade off between these two opposing aspects to prepare macrocycles not from many nor from one but rather from two larger building blocks. This clearly does not give optimal cyclization yields but keeps the overall synthetic effort in reasonable dimensions.

The reactivity of the end groups has a strong influence on the cyclization yields. Only if the reaction between them is fast, the seldom occasions when the precursor chain ends happen to be at close distance will be optimally exploited. Otherwise linear growth will be even given a greater chance. For example, Henze used a Sonogashira reaction to build bipyridine macrocycles. He observed that when arylbromides were used in ring closure reactions, no cycle but rather linear oligomers formed. In contrast, when the exact same sequence was performed with aryliodides the cyclic compound was obtained in yields of 20-30% which is the normal range for the approach from two "halves".[17a] The same was obtained by Hensel, who found that ring closure based on Suzuki cross-coupling is much inferior when arylbromides are used instead of aryliodides.[4]

Though one would expect pseudo high dilution conditions help the cyclization, there are cases where this does not seem to be so. Henze applied pseudo-high dilution conditions for cyclization reactions to bipyridine containing macrocycles, but the yields were surprisingly low. Better results were obtained when all components were put together from the beginning at concentrations of 0.0015 mol/l.[17] This finding which is not exceptional in this area is difficult to understand but may have an experimental background. Pseudo high dilution conditions are normally created by the use of syringe pumps which at a very low rate supplies the reaction vessel with the cyclization precursor. Such set ups are difficult to keep strictly under inert atmosphere. Oxygen may therefore have entered the reaction and influenced its outcome in a detrimental way.

Two different cyclization reactions and two different approaches (Route b and c, Chapter 3.1., p 10) were used in the present work for the construction of bipyridine macrocycles: a Sonogashira reaction as well as an acetylene-acetylene oxidative coupling of one or two ring precursors.

4.3.1. Ring closure reactions by Sonogashira-Hagihara cross-coupling of two building blocks

One of the objectives of the present work was to make bipyridine macrocycles which do not differ in ring size, but rather in their substitution pattern and number of bipyridine units (Figure 37). This pattern plays an important role with regard to various properties, for example: solubility, aggregation, and potential for chemical modification. The macrocycle **E1** with six hexyl groups, e.g., should have a good solubility in common organic solvents and show interesting aggregation in solids and/or in melts. Macrocycle **E2** with its one THP protected alcohol group is attractive for its further conversion into macromonomers in order to provide access to polymers with pendent macrocycles. Macrocycle **E3** contains one bipyridine (instead of the normally used two) and serves as model compound for supramolecular constructions. Additionally, it may present interesting packing in single crystal or in melts.

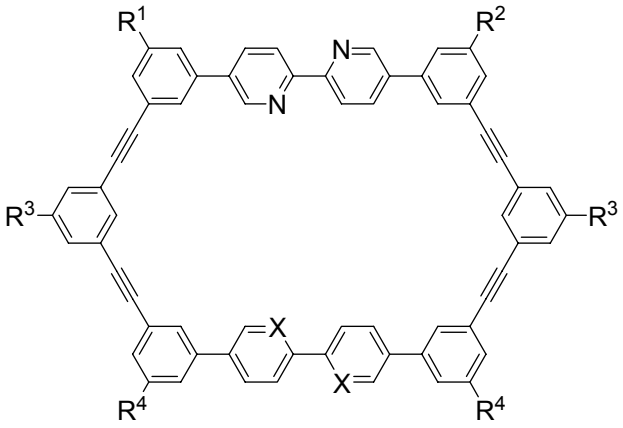

E1: $R^1 = R^2 = R^3 = R^4$ = Hex, X = N
E2: R^1 = THP, $R^2 = R^3 = R^4$ = Hex, X = N
E3: $R^1 = R^2 = R^3 = R^4$ = Hex, X = CH
E4: $R^1 = R^2$ = THP, $R^3 = R^4$ = Hex, X = N
E5: $R^1 = R^2 = R^4$ = THP, R^3 = Hex, X = N

Figure 37. Bipyridine macrocycles with different substituent pattern.

E4,[57] with its two THP groups, is attractive as source for unconventional diols for polyesters, polyamides, and alike, and, finally, **E5**[17b]for its decoration with dendrons, self-recognizing and/or polymerizable groups, the latter of which would potentially be useful for covalent stabilization of cylindrical cycle stacks by solid state polymerization similar to Ringsdorf's[66] and Gadhiri's work.[67] The syntheses of the first three macrocycles **E1**, **E2**, and **E3** are described in this chapter, the other macrocycles **E4** and **E5** were already obtained before by Henze and are therefore not treated here.[17]

4.3.1.1. Syntheses of macrocycles 103a-c

The macrocycles **103a-c** were prepared by a Sonogashira cross-coupling of two different ring precursors (half rings) one of which carries the iodo functionality (a bisfunctionalized bipyridine or a quaterphenyl unit) and the other the acetylene.[17] Scheme 42 shows how by combining various building blocks with different substituent patterns a whole variety of macrocycles could accessed. For example, cycles **103a, 103b**, and **103c** were prepared from **102a** and **76**, **102b** and **76**, and **102a** and **83**, respectively. The synthesis of the cycle precursors was already described in Chapter 4.2. High dilution conditions were used in order to favour the cyclization over oligomerization. The cyclizations were done using Henzes procedure.[17] A heavy-walled flask was charged with the ring precursors in a mixture of toluene/TEA 1:1 with a molarity of 0.0015 M. The flask was degassed and flushed with nitrogen two times. Then $Pd(PPh_3)_4$ and CuI (0.04 equiv) were added and the flask was degassed once more and sealed with a Teflon screw cap. This mixture was stirred at 60 °C for 4 days and then at 90 °C for one day. The solvent was removed

and the residue dissolved in DCM and treated with a solution of KCN in order to remove the Cu and Pd ions. The product was then freeze dried from dioxane or benzene and analysed by gel permeation chromatography (GPC).

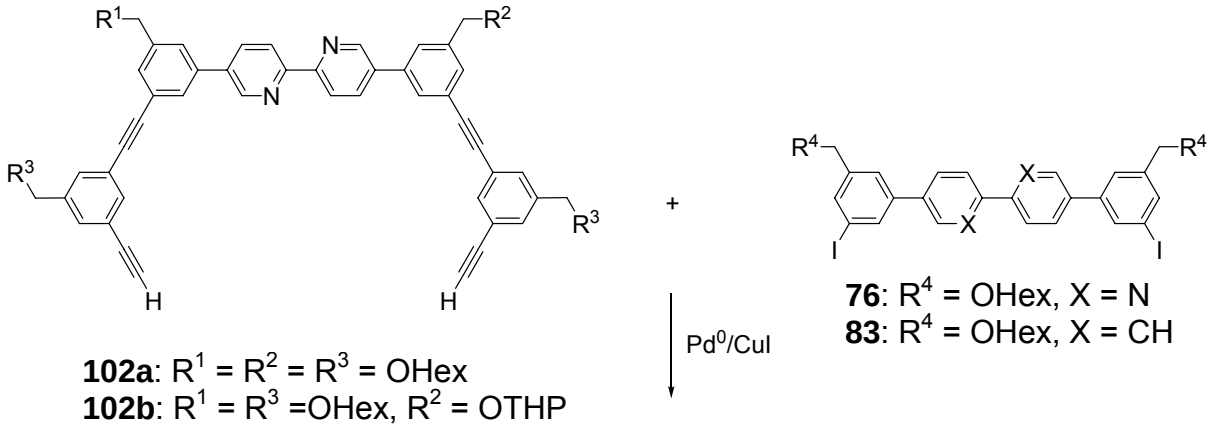

102a: $R^1 = R^2 = R^3$ = OHex
102b: $R^1 = R^3$ =OHex, R^2 = OTHP

76: R^4 = OHex, X = N
83: R^4 = OHex, X = CH

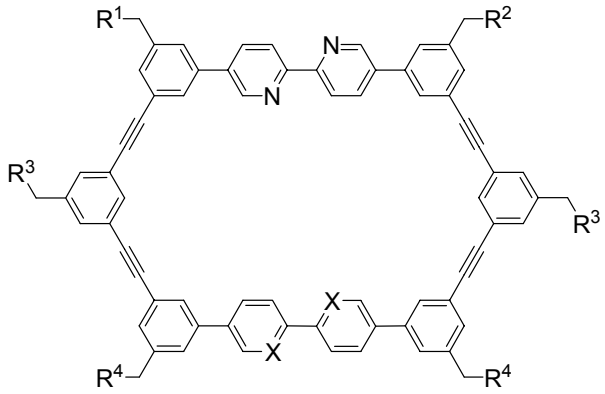

103a: $R^1 = R^2 = R^3 = R^4$ = OHex, X = N
103b: R^1 = OTHP, $R^2 = R^3 = R^4$ = OHex, X = N
103c: $R^1 = R^2 = R^3 = R^4$ = OHex, X = CH

102a + 76 ⟶ 103a
102b + 76 ⟶ 103b
102a + 83 ⟶ 103c

Scheme 42. Synthesis of bipyridine macrocycles **103a-c**.

GPC normally showed three different signals at retention times of ca. 13.1, 13.8 and 14.7 minutes, and a higher oligomeric material between 10 and 13 minutes. Figure 38 depicts the GPC traces of the raw products of macrocycles **103a-c**.

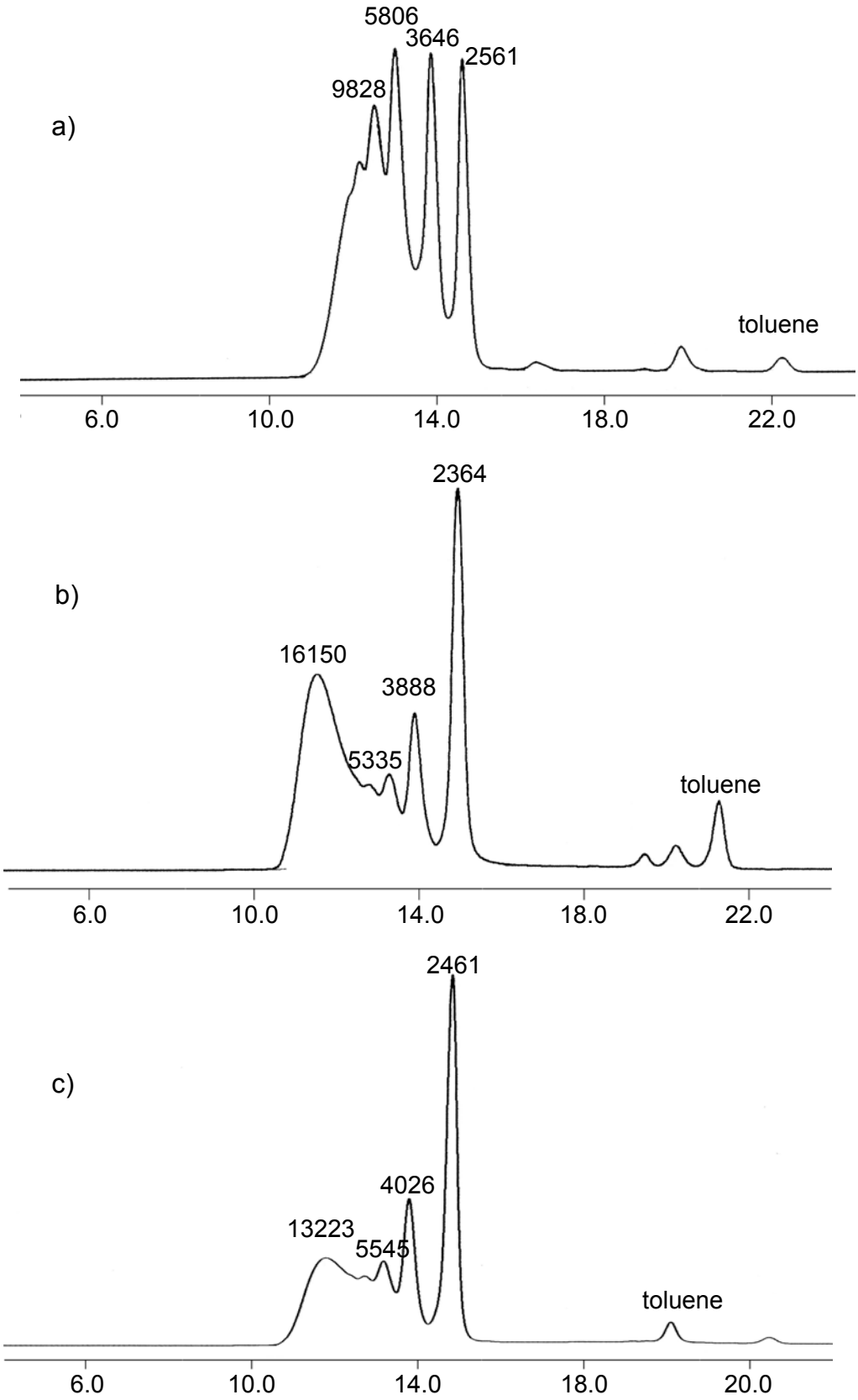

Figure 38. Raw mixture GPC traces of the macrocycles' **103a** (a), **103b** (b), and **103c** syntheses (c).

In the beginning the cyclization reactions were done with relatively small amounts of ring precursors. In the course of this work, cyclizations were scaled up in order to provide macrocycles in larger quantity for subsequent studies. By this scaling-up it was observed that the cyclization yields tended to decrease (Table 2). The reason for this is not yet clear. The macrocycles were obtained in yields of 18-35% on the 100-900 mg scale after purification by GPC.

Table 2. Yields of isolated macrocycles **103a-c** from different experiments.

Macrocycle	mmols of ring precursors used	yield %
103a	0.13	35
	0.3	18
103b	1.8	23
	2.0	22
103c	0.5	28
	1.0	21

The two sharp signals at longest elution time were isolated by preparative GPC. Sometimes the fractions obtained this way did not contain pure material. In these cases additional purification steps by conventional column chromatography were applied which in most cases provided analytically pure products. Occasionally the large amount of solvent required for preparative GPC caused additional problems in that unknown impurities in the solvent were enriched the cycle fractions. These impurities had a characteristic signal in the ^{1}H NMR spectrum at δ = 5.5 ppm. In these cases the fraction was dissolved in the smallest possible amount of THF and precipitated with methanol, followed by centrifugation of the fine precipitate.

With the help of NMR spectroscopy and mass spectrometry the compounds which caused the two peaks in the GPC were assigned as cycles **103a-c** and another compound with double molecular weight **[103a-c]$_2$**. This was based on the NMR spectroscopical evidence that no end groups were present and a mass spectrometric analysis. Thus, the precursor's **102** sharp singlet at δ = 3.3 ppm disappeared in the products ^{1}H NMR spectrum as did the precursor's **76** (or **83**) C-I group at δ = 95 ppm in the ^{13}C NMR spectrum. Figure 39 compares the ^{1}H NMR spectra of ring precursor **102b** and macrocycle **103b** to illustrate this point.

Because of the macrocycle's high symmetry point group the ^{1}H NMR spectrum of **103a** is simple, displaying seven aromatic proton resonances with the expected coupling patterns between δ = 9.0 and 7.4 ppm (Figure 40).

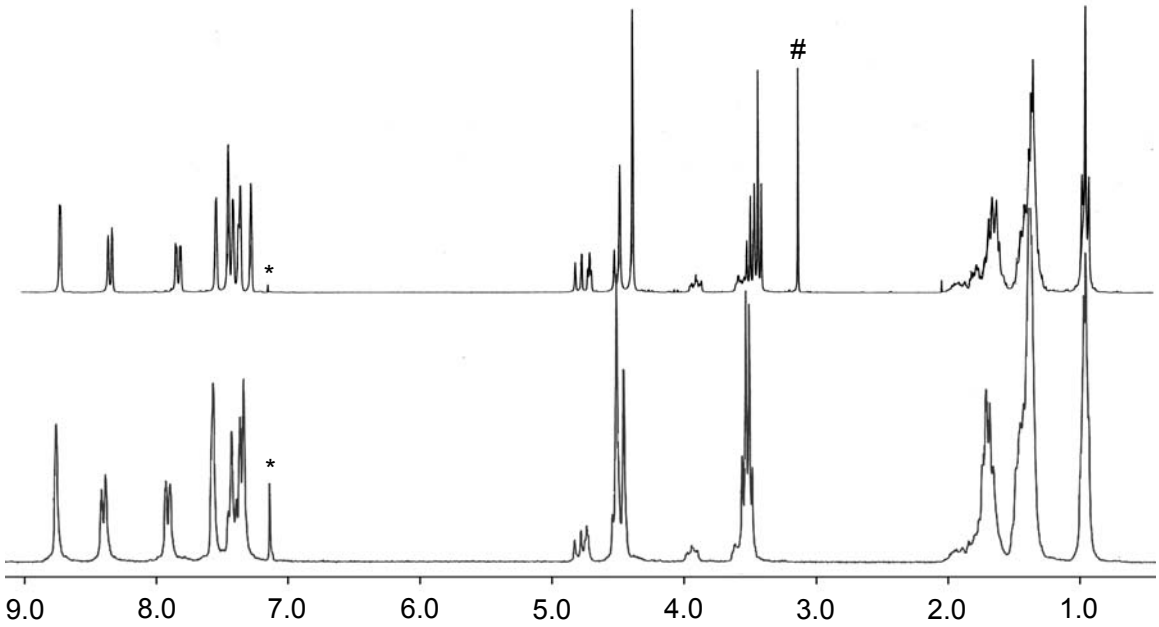

Figure 39. ^{1}H NMR spectra of ring precursor **102b** (a) and macrocycle **103b** (b). The acetylenic end group of **102b** is marked (#) (*: $CDCl_3$, 250 MHz, 20 °C)

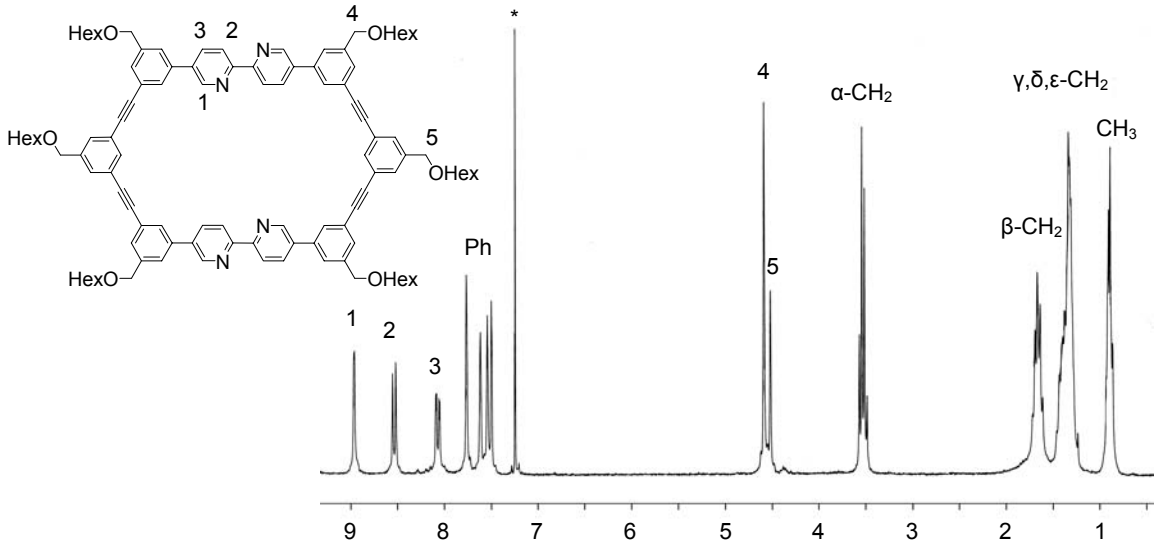

Figure 40. ^{1}H NMR spectrum of **103a** with signal assignment (*: $CDCl_3$, 250 MHz, 20 °C).

The FAB mass spectra of **103a-c** were recorded in MNBA/DMSO/CH_2Cl_2 and display peaks at *m/z* values which correspond the molecular ions. They also show other

peaks due to fragmentation or adduct formation which were easily assigned (Figures 41-43).

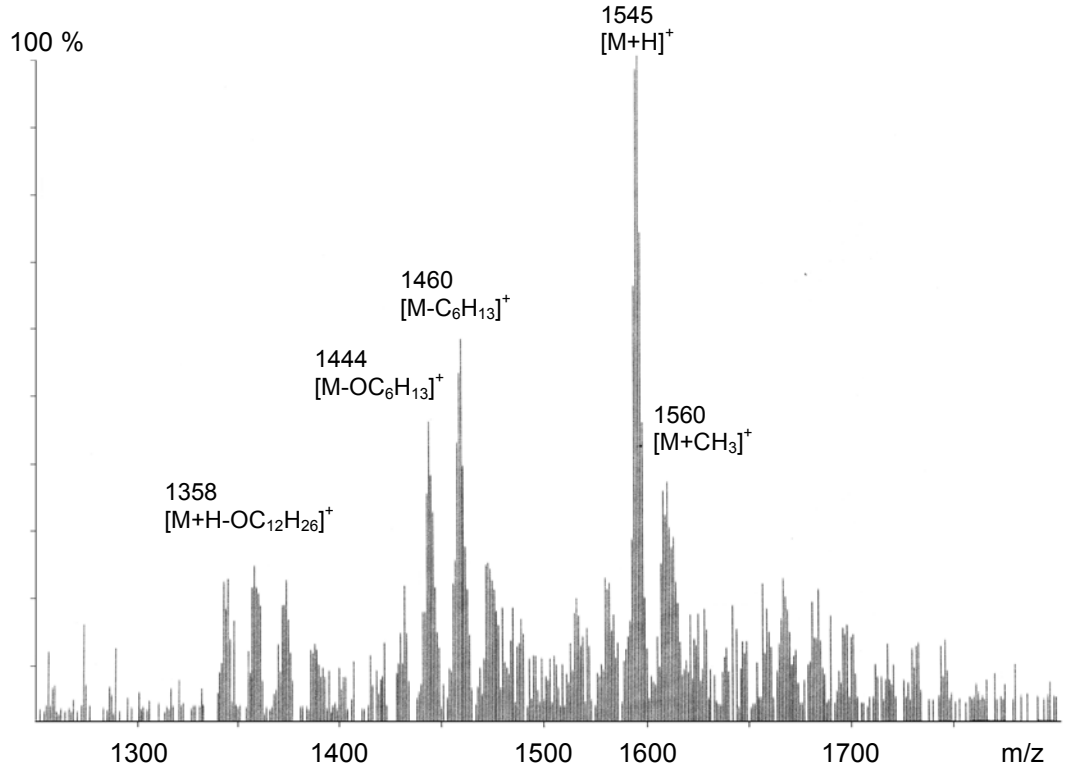

Figure 41. FAB(+)-MS spectrum of macrocycle **103a**.

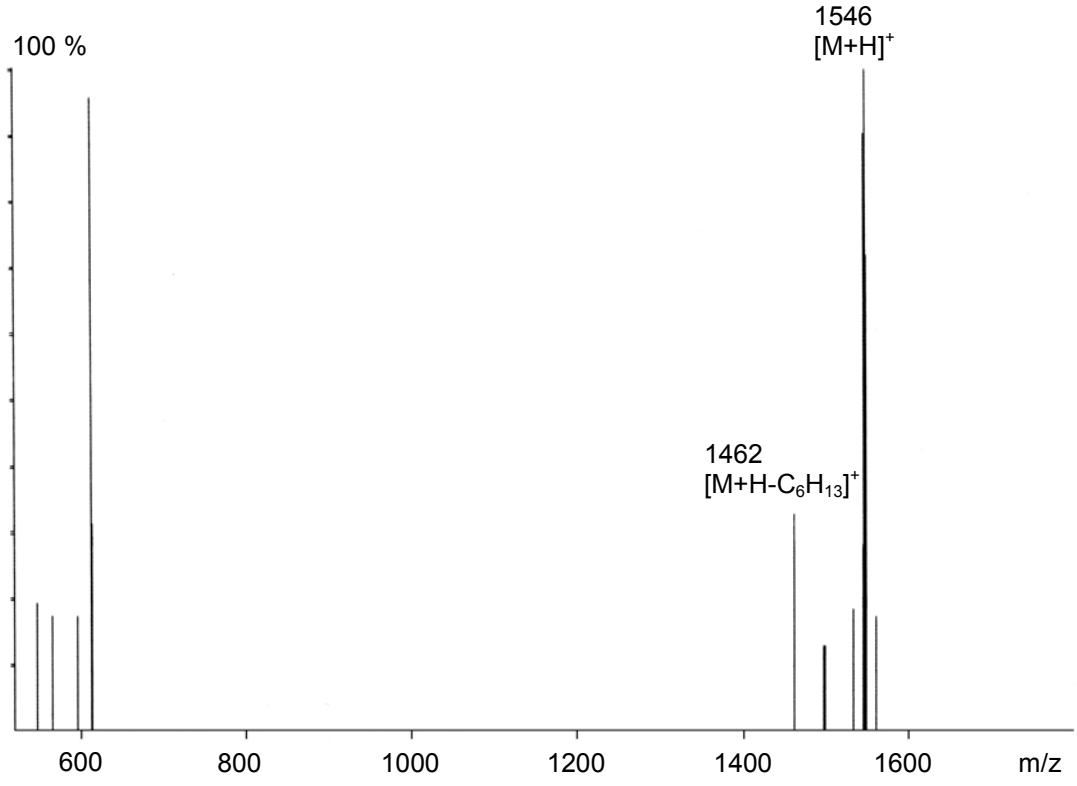

Figure 42. FAB(+)-MS spectrum of macrocycle **103b**.

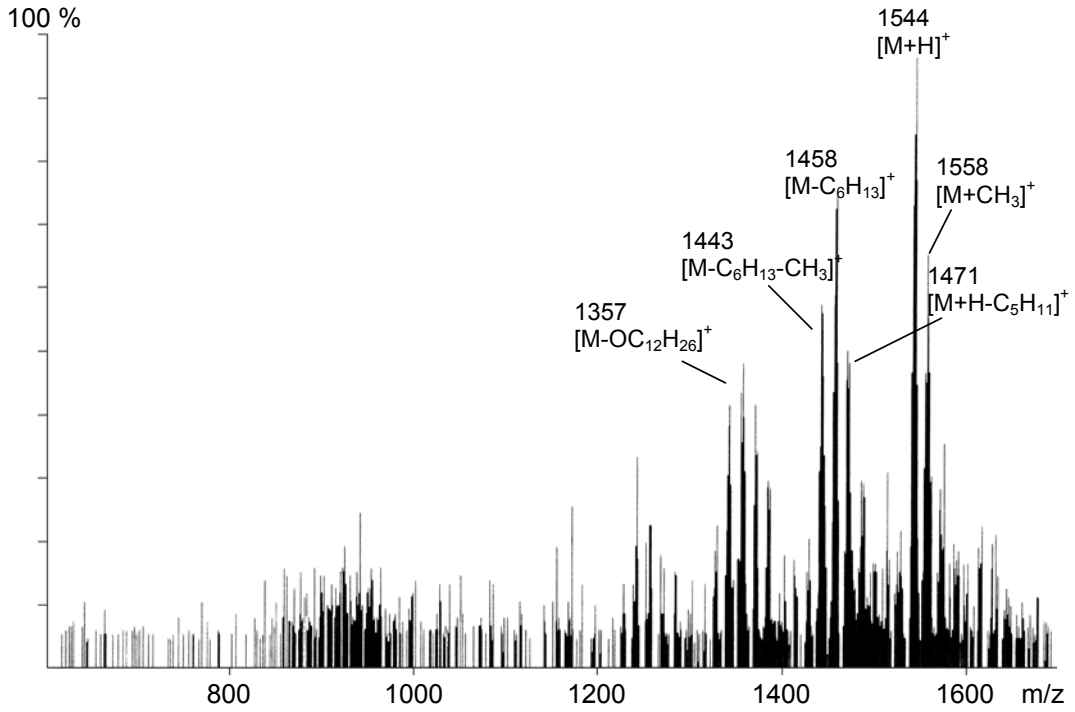

Figure 43. FAB(+)-MS spectrum of macrocycle **103c**.

A small quantity of oligomers with the double molecular weight **[103a-c]$_2$** were isolated and partially characterized. There are two obvious structure proposals which explain the observed double molar mass. Either the compounds are just larger macrocycles or consist of two intertwined macrocycles of kind **103a-c** with catenane topology.[68,69] It is quite difficult to differentiate between these options without having single crystal X-ray analysis at hand. The ^{1}H and ^{13}C NMR spectra of compounds **[103a-c]$_2$** are very similar with those of the cycles **103a-c** and can thus not be used here. Compounds **[103a]$_2$** and **[103c]$_2$** were analyzed by the MALDI-TOF mass spectrometry. The spectra show peaks at *m/z* = 3089.7 and 3086.88, respectively, which are in fact double the molar masses of the corresponding cycles **103a** and **103c** (Figures 44 and 45).

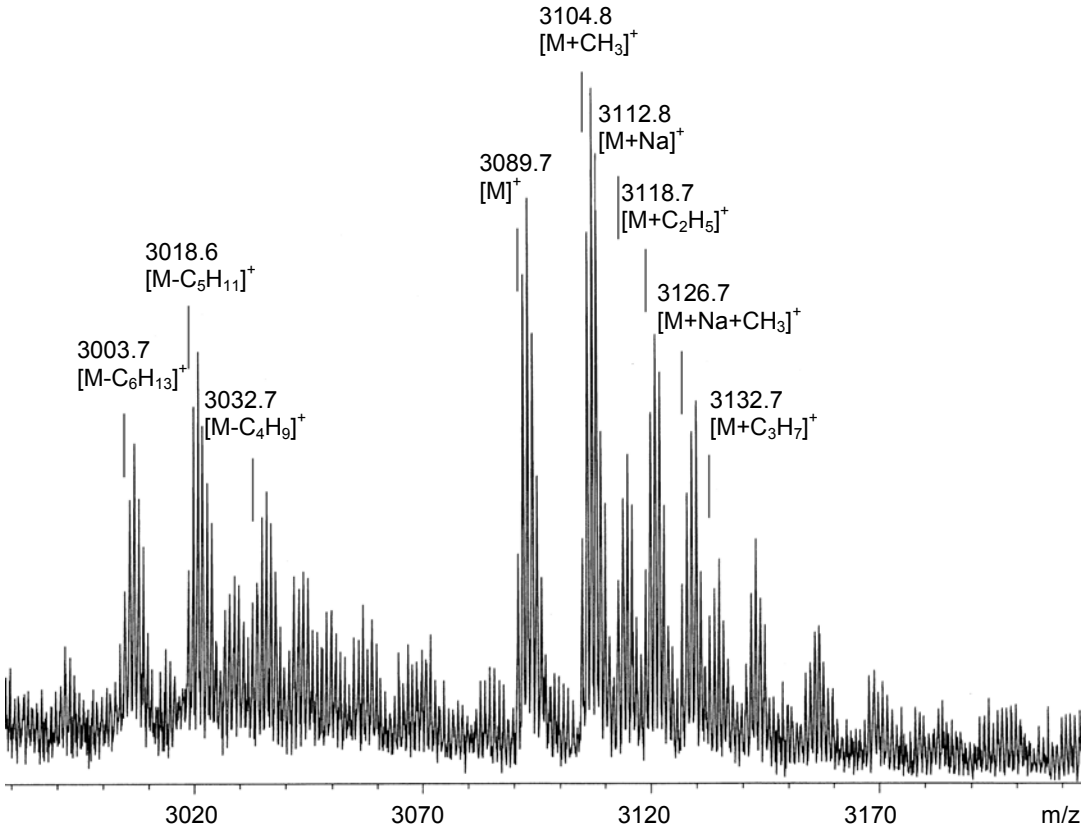

Figure 44. MALDI-TOF mass spectrum (reflector mode, dithranol matrix) of compound **$[103a]_2$.**

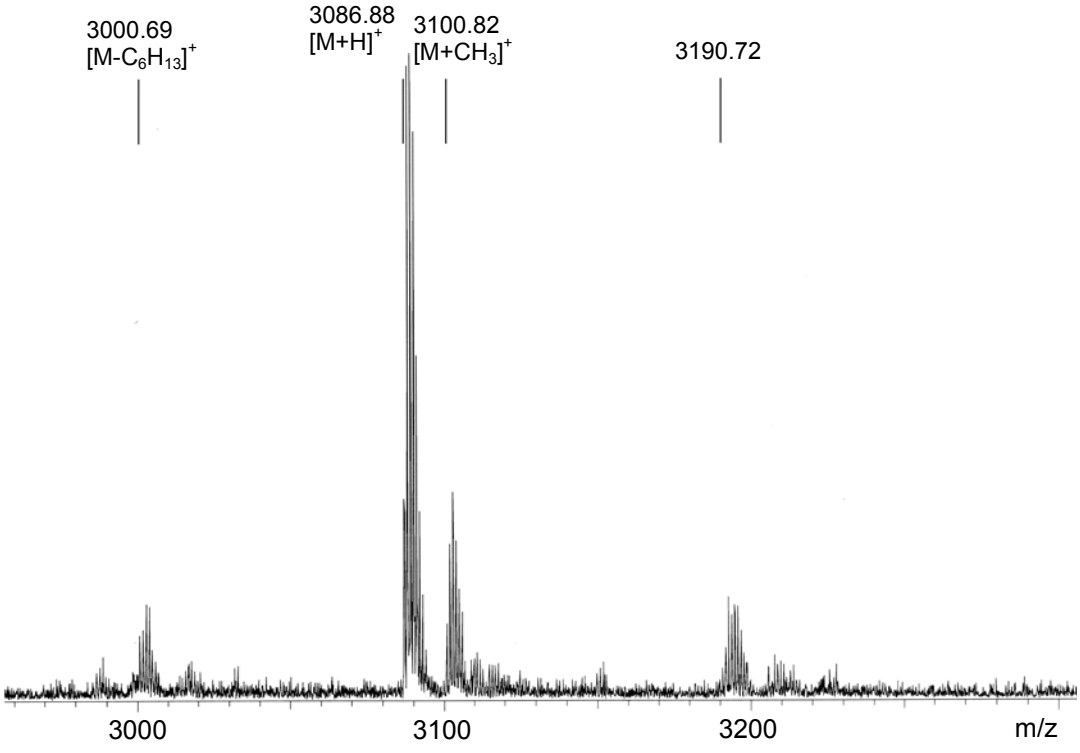

Figure 45. MALDI-TOF mass spectrum (reflector mode, dithranol matrix) of compound **$[103c]_2$.**

4.3.1.2. Synthesis of macrocycle 10

Herein, a new route to the known macrocycle **10** is described (Scheme 43). It was prepared before by Henze from two building blocks of kind **C** and **D** (Chapter 3.1., Scheme 5, p. 12). The new synthesis is based on the commercial availability of TMSA and 1,3-diiodobenzene and has a reduced number of steps from 17 to 13. The macrocycle was constructed from two building blocks **100b** and **100c** which were reacted using standard procedures as described before (Scheme 43). The GPC trace of the raw product mixture (Figure 46) was similar to those observed for other macrocyclizations (Figure 38, p. 71). Macrocycle **10** was isolated by preparative GPC on the 540 mg scale in 28% yield.

The main advantages of the new route are the reduction of steps and an easier purification of compounds. Macrocycle **10** was used for the synthesis of Ru and Os complexes.

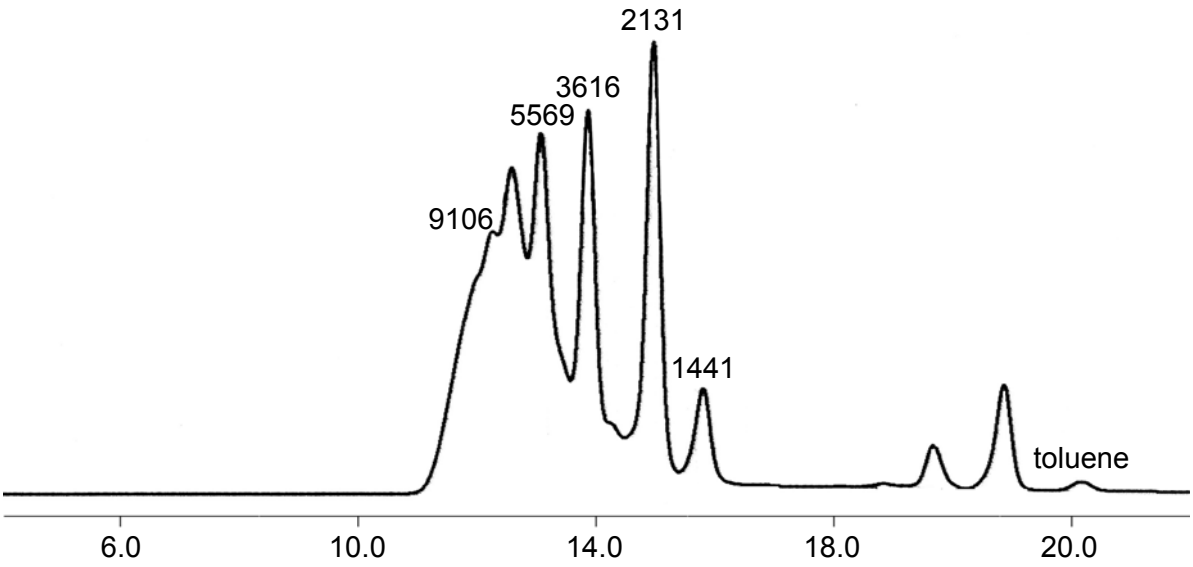

Figure 46. GPC trace of the raw cyclization product obtained from reaction of **100b** with **100c**. The signal at 2131 represents the macrocycle **10**.

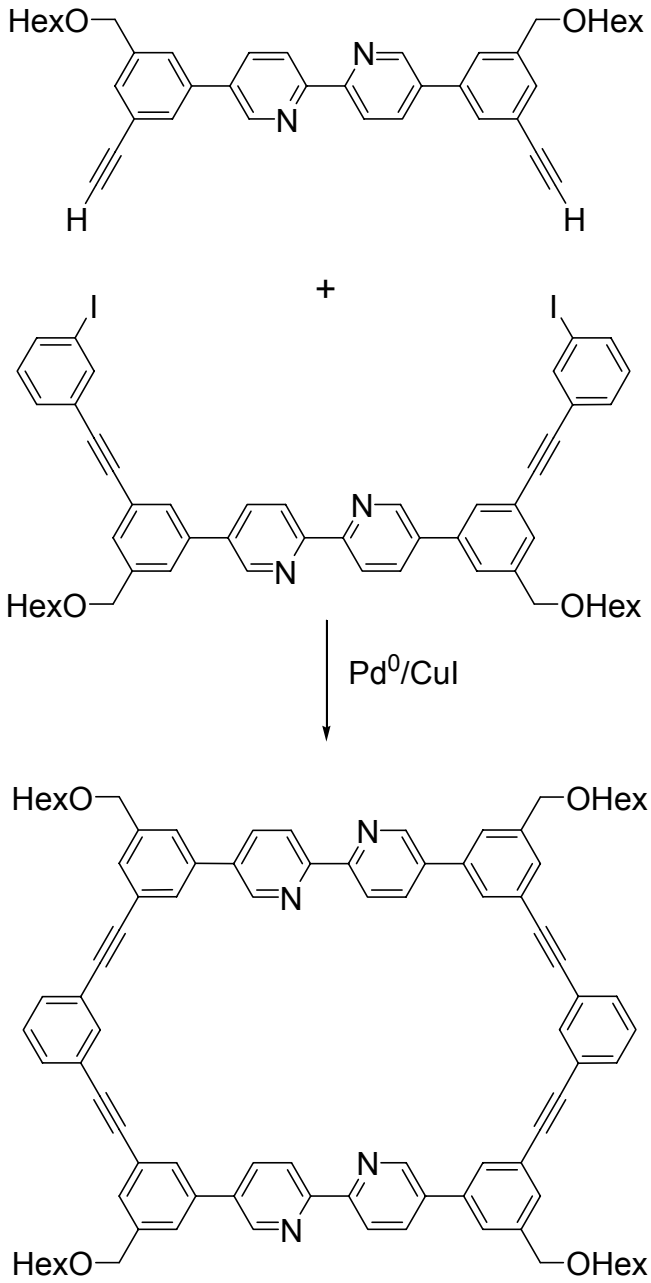

Scheme 43. Synthesis of macrocycle **10** from **100b** and **100c**.

4.3.1.3. Synthesis of the macrocycle 103d

Tilley used zirconocene induced coupling reactions starting from functionalised diynes for the synthesis of bipyridine containing macrocycles and obtained them in both large quantities and high yields.[39] When equimolar amounts of $Cp_2Zr(py)(Me_3SiC\Xi CSiMe_3)$[70] and trimethylsilyl protected diynes were mixed in benzene, crystals of **57** precipitated in yields of 95% (Scheme 44). Inspired by this, it was considered interesting to find out whether a shape persistent bipyridine macrocycle properly decorated with silyl-substituted diynes (**103e**) could possibly cyclize and lead to a huge trimeric cycle **103f** (Scheme 44). This would provide

access to cage with unprecedented structure. Compound **103f** contains 12 bipyridine units which could be used for further functionalization.

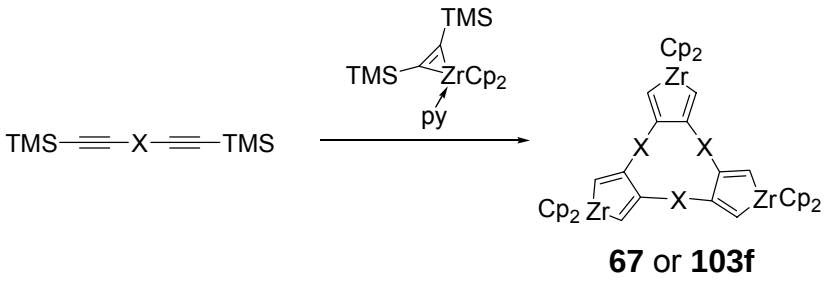

67 or **103f**

67: X =

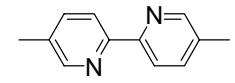

103f: X =

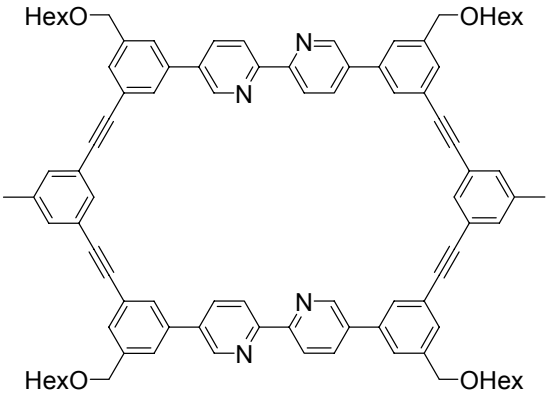

Scheme 44. Synthesis of macrocycle **57** and the proposed analogy leading to cage **103f** using the zirconocene-coupling reaction of diynes.

In order to test whether the Tilley protocol can be applied to the synthesis of such a complex target like **103f** it was necessary to first prepare a macrocycle which contains in “para”-position two acetylenic units. Macrocycle **103e** was considered an interesting first target. Its synthesis is illustrated in Schemes 45 and 46. The sequence starts with **103d** which was obtained from two different precursors **76** and **102c** (Scheme 45). They were brought in reaction according to the protocol described before. The raw product was soluble in DCM, THF, and toluene and was analysed by analytical GPC. The GPC elution curve was similar to that obtained for the other cyclization experiments. Two ring closure reactions to macrocycle **103d** were performed on the 0.13 and 0.88 mmol scale. Like in the previous cases, a decrease in cyclization yields was observed for the larger scale experiment. The values dropped from 26 to 16%, respectively. Figure 47 displays the GPC elution curves of these two experiments to illustrate this decrease.

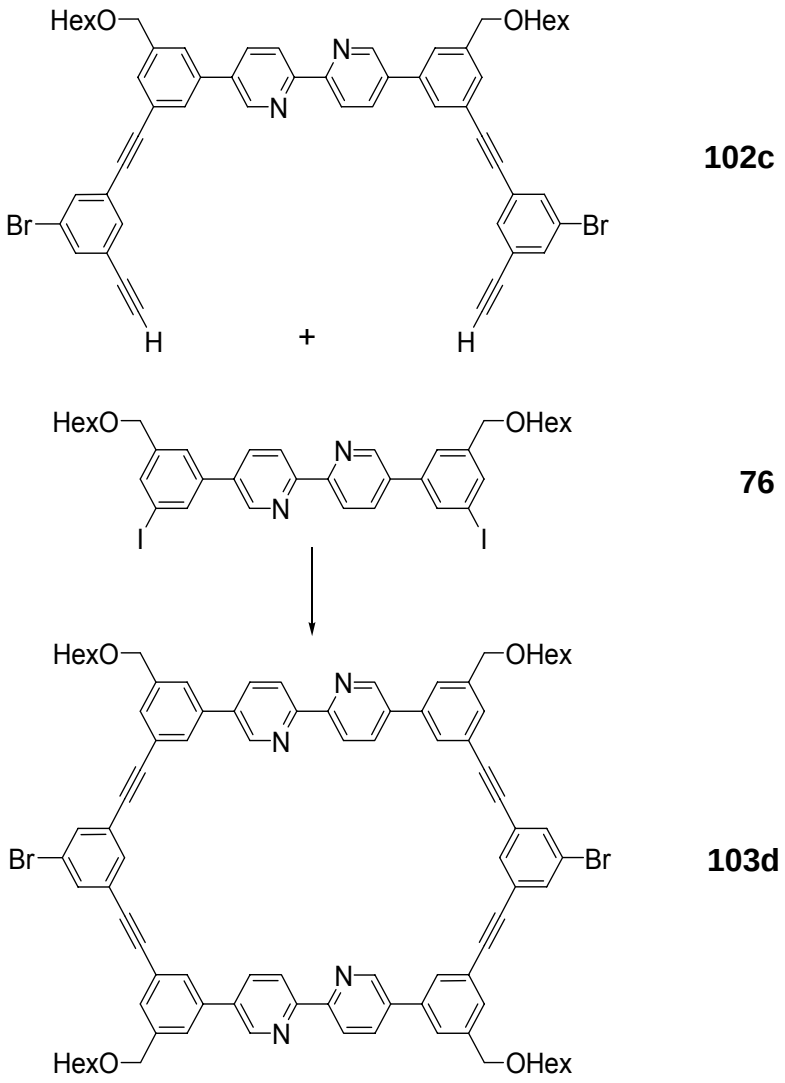

Scheme 45. Synthesis of macrocycle **103d** from **76** and **102c**.

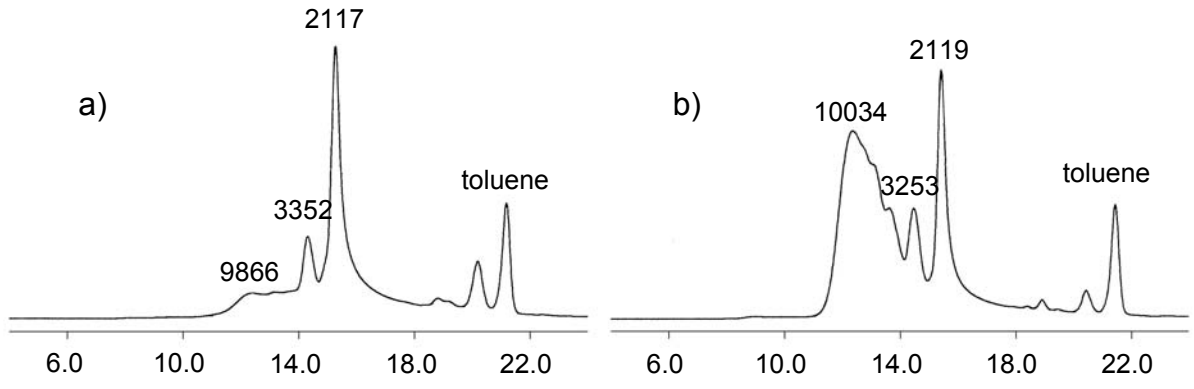

Figure 47. GPC traces of the raw cyclization product for the two experiments to **103d** with 0.13 mmol (a) and 0.88 mmol of ring precursors (b).

The cycle **103d** was isolated by preparative GPC. It was poorly soluble in common organic solvents like DCM, chloroform, benzene, toluene, and THF. A ^{1}H NMR spectrum could still be recorded in toluene at 80 °C, for a ^{13}C NMR spectrum, however, the solution could not be obtained concentrated enough. In the ^{1}H NMR spectrum no signal of the free acetylene was detected, indicating that the compound was actually a macrocycle rather than on open chain oligomer. The MALDI-TOF mass spectrum recorded in dithranol supports the macrocycle formation. It shows a signal at *m/z* = 1473.2 which corresponds to $[M+H]^+$ (Figure 48).

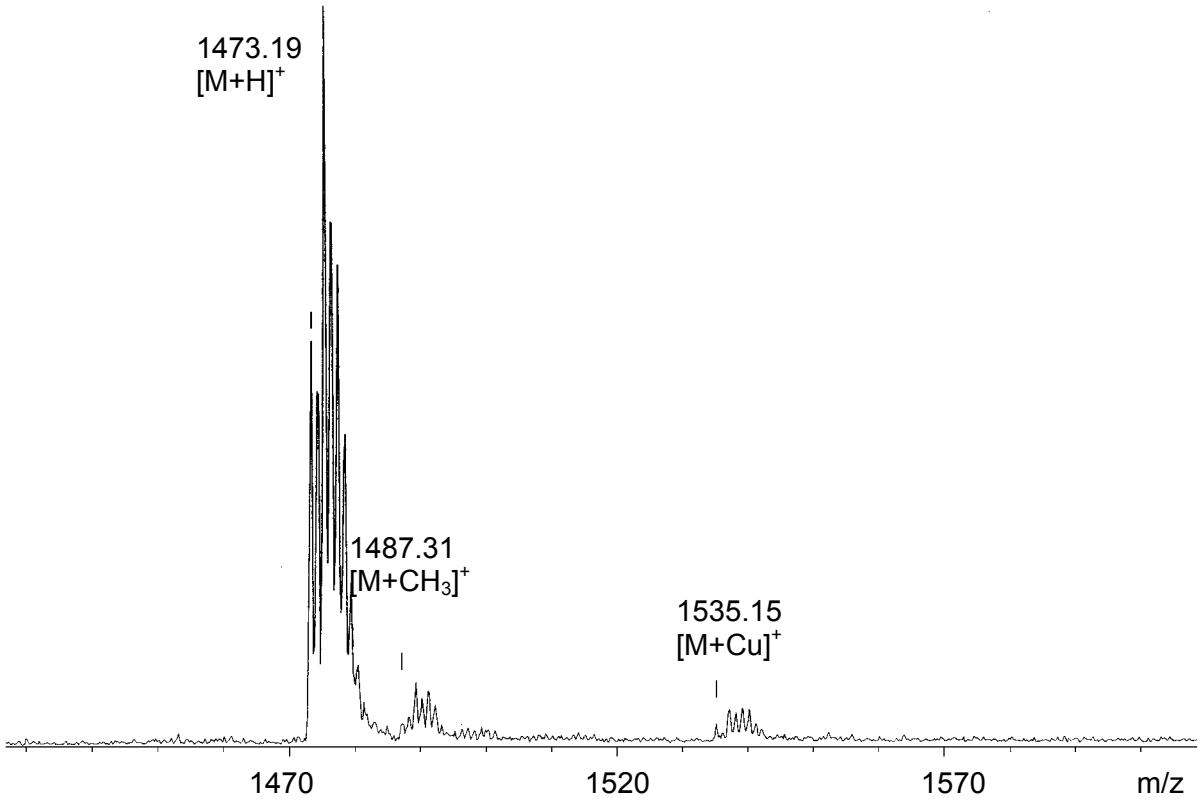

Figure 48. MALDI-TOF mass spectrum of **103d** in dithranol (linear mode).

In the next step the dibromide **103d** needed to be converted into its bisacetylenic derivative **103e** carrying the acetylenes in a protected form. It was obtained from a Sonogashira cross-coupling between **103d** and an excess of TMSA (Scheme 46). After column chromatographic purification the ^{1}H NMR spectrum of **103e** showed six signals in the aromatic part. The integration of the characteristic signal of the TMS groups at δ = 0.27 corresponds to 18 protons (Figure 49) which was the easiest measure to make sure that both bromides had actually reacted.

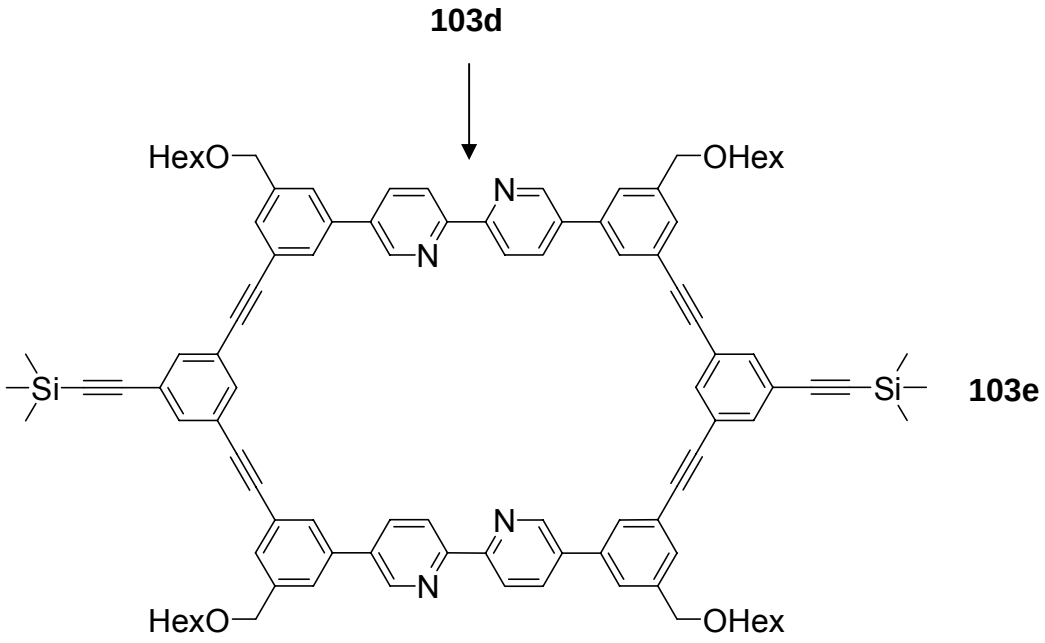

Scheme 46. Synthesis of macrocycle **103e** by a Sonogashira reaction between **103d** and TMSA

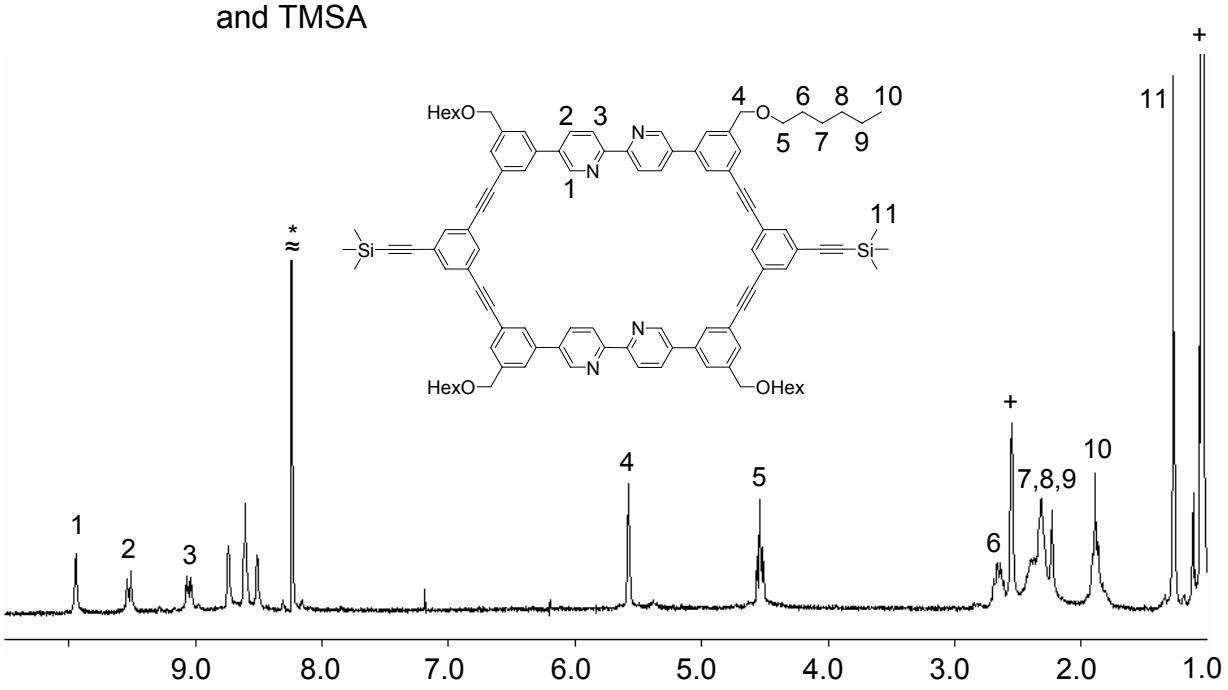

Figure 49. ^{1}H NMR spectrum of macrocycle **103e** with signals assigned (*: $CDCl_3$, 250 MHz, 20 °C).

The FAB mass spectrum shows a signal at *m/z* = 1511.7 which was assigned to $[M+H]^+$ of the macrocycle as well as other characteristic signals for the fragmentation (Figure 50). No signal was detected at *m/z* = 1475.5, which is the mass of the starting macrocycle **103d** as well as at *m/z* = 1491.6, which is the mass of the partially

coupled macrocycle (not shown). Unfortunately, the small amount of macrocycle **103e** which was obtained was not large enough to do the final cyclization experiment. A scale-up of the sequence which should be feasible could unfortunately not be performed within the timeframe of the present thesis.

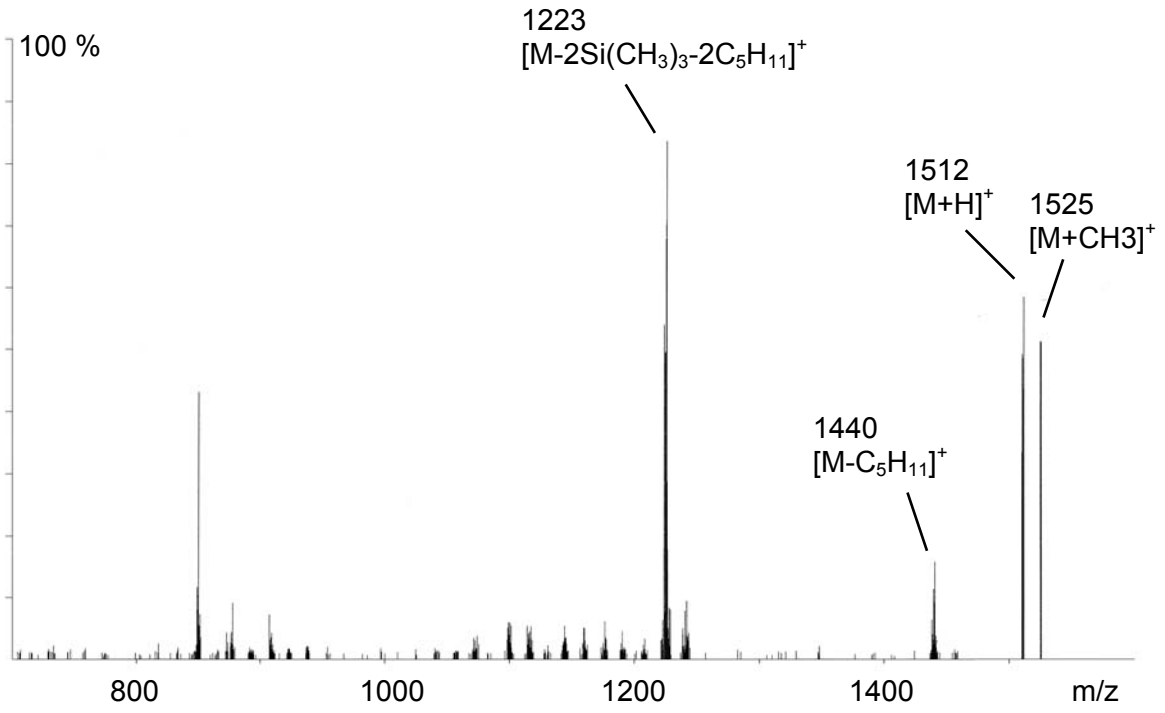

Figure 50. FAB (+)-MS spectrum of macrocycle **103e**.

4.3.2. Ring closure reactions by Sonogashira-Hagihara cross-coupling of one cycle precursor

So far, the bipyridine macrocycles were constructed from two building blocks in 20-30% yields. These relatively low yields are compensated by a relatively easy synthetic access to the respective building blocks. One disadvantage of this approach can be seen in the difficulty to place various functional groups at certain positions on the macrocycle. Thus, this chapter describes the first ever synthesis of a bipyridine macrocycle from a single precursor compound which additionally allows for a controlled placement of functional groups at predetermined positions of the cycle. This latter aspect is important, for example, for the use of cycles in energy and electron transfer studies, as switches, and alike. Finally from hydrocarbon cycle synthesis it was to be expected that the cyclization yields for such an approach should be much higher and possibly in the range of 65-75 %. It was clear from the

beginning that the price to be paid for these advantages would be the large number of steps. This turned to be in fact the case. A high synthetic effort needed to be invested in cycle precursor **88d**, whose synthesis was accomplished in 21 steps (Chapter 4.2.4., Schemes 35 and 36). The non-symmetrical building block **85** played a key role in the sequence. Its synthesis was done as described before (Chapter 4.2., Scheme 35, p. 56). A series of Sonogashira-type coupling reactions with various silylprotected acetylenes (TMSA and TIPS) followed all the way through to **88d**, the direct cycle precursor. All these procedures went smoothly and were high-yielding. Compound **88d** was isolated on the 250 mg scale. Two different functional groups on the ring precursor were introduced at defined positions: a THP and an ester group (Scheme 47) at the "para" positions. These groups were chosen so that they can be selectively addressed with minimum synthetic effort after the cycle is formed.

For the ring closure reaction pseudo high-dilution conditions were applied. A solution of precursor **88d** was syringed during 36 h into a refluxing mixture of Pd^0/CuI in toluene/triethylamine (Scheme 47).

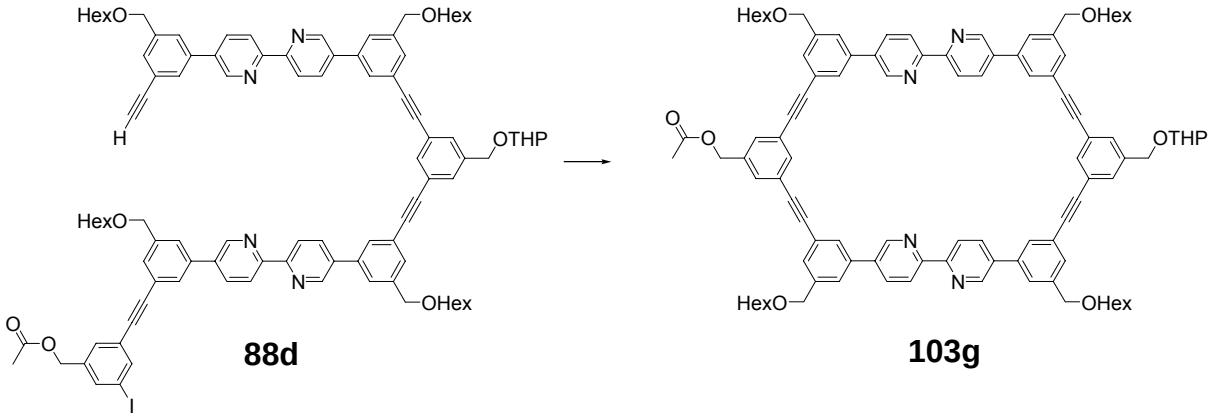

Scheme 47. Synthesis of the macrocycle **103f** from the direct cycle precursor **88d**.

The raw product was analysed by GPC. The elution curve showed four peaks. The isolation of the products was achieved by preparative GPC. Two of them could be identified. One isolated compound (a very small amount) came at retention times which are characteristic for the cycle and was found to be the desired macrocycle **103g**. The MALDI-TOF mass spectrum showed signals at *m/z* = 1503.5, 1565.5, and 1606.5. The first two were assigned as $[M+H]^+$ and $[M+Cu]^+$. The last one could not yet be assigned with certainty. It may indicate a Pd complex which would be expected at *m/z* = 1609 (Figure 51).

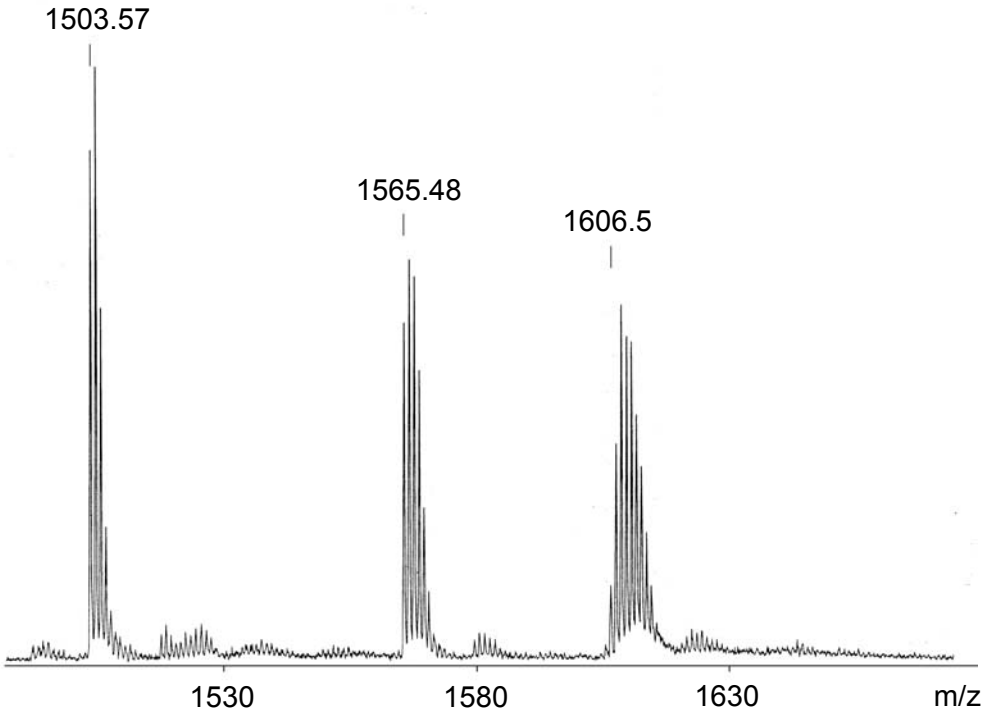

Figure 51. MALDI-TOF mass spectrum (dithranol matrix, reflector mode) of macrocycle **103g**.

The second isolated compound came at expected retention time which corresponds to the double molecular weight macrocycle **[103g]$_2$**. However, the ^{1}H and ^{13}C NMR spectroscopy as well as MALDI-TOF mass spectrometry proved that this compound was not **[103g]$_2$** but rather a side product **104** (Figures 52 and 53). The lower concentration of the ring precursors and the long reaction time was detrimental for cycle formation and a side acetylene-acetylene dimerization reaction of **88d** to **104** occurred (Scheme 48).

Even if the macrocycle **103g** was not obtained in reasonable quantities, it was nevertheless shown that controlled functionalization of bipyridine containing macrocycles can be achieved and also the direction future for such cycles.

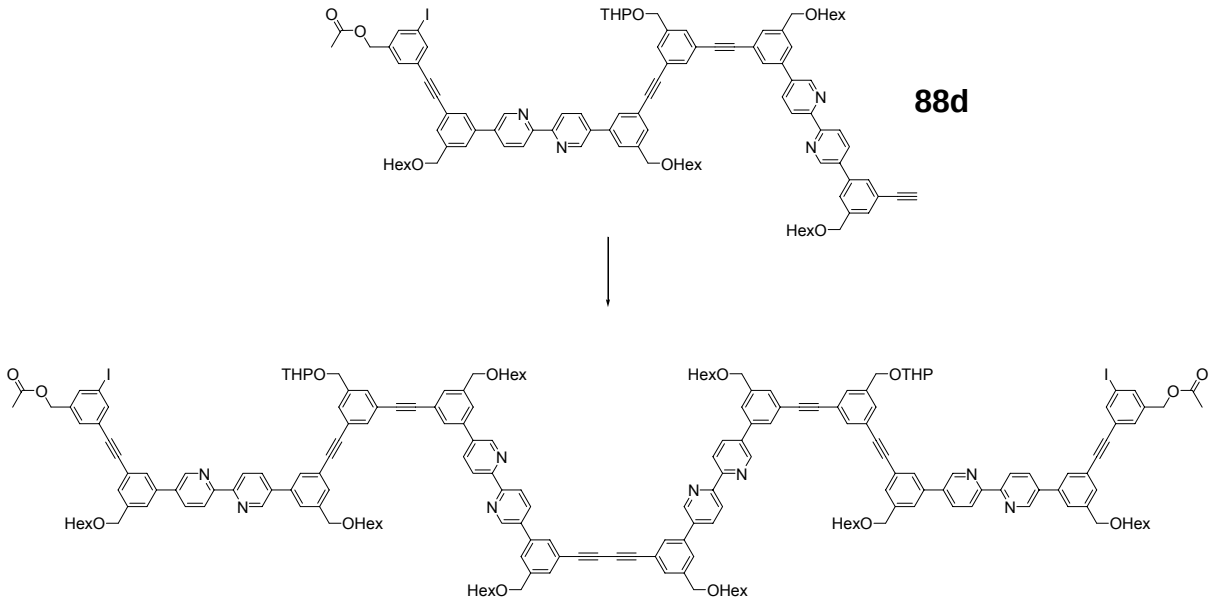

Scheme 48. Acetylene-acetylene dimerization of the ring precursor **88d** to give **104**.

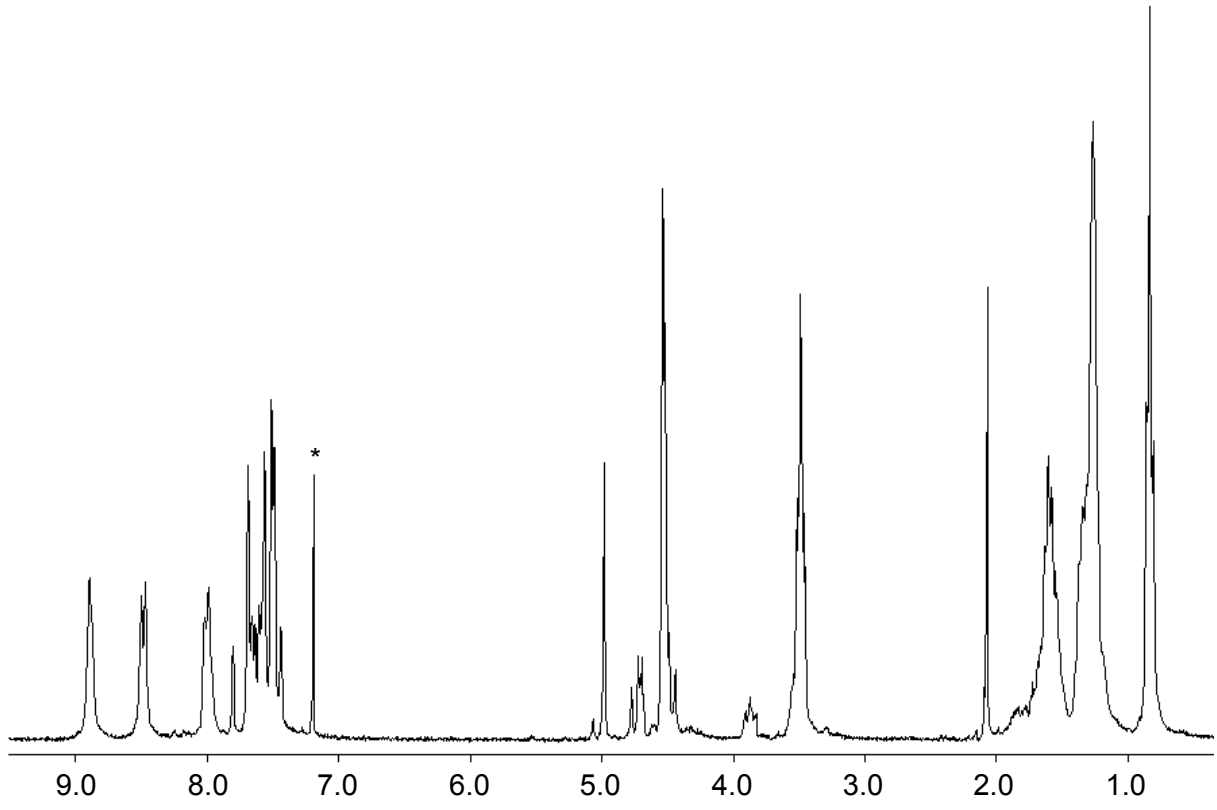

Figure 52. ^{1}H NMR spectrum of the side product **104** (*: $CDCl_3$, 270 MHz, 20 °C).

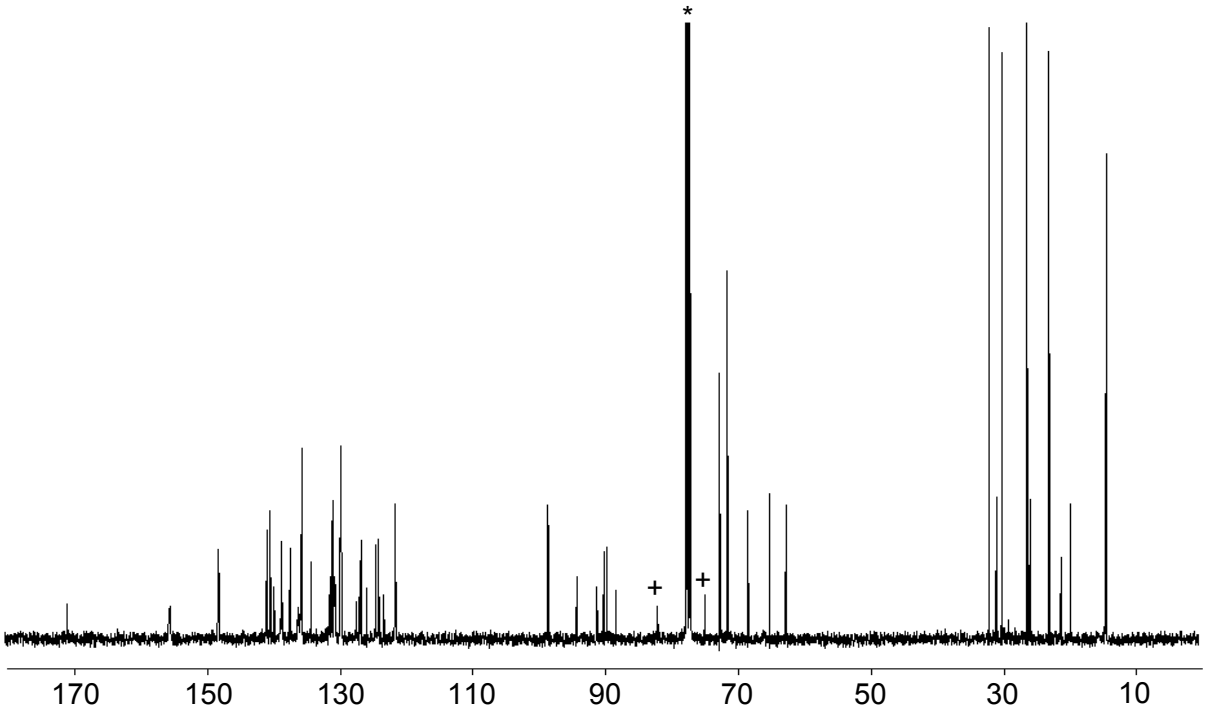

Figure 53. ^{13}C NMR spectrum of the side product **104** (*: $CDCl_3$, 63 MHz, 20 °C, + the two additional acetylene C signals which could not be assigned to **[103g]$_2$** but rather to **104**).

4.3.3. Ring closure reactions by oxidative acetylene coupling

The oxidative acetylene dimerization has oftenly been used in ring closure reactions. Hydrocarbon macrocycles as well as heteroaromatic macrocycles with different sizes and substituent patterns have been prepared using this reaction (see Table 1, Chap. 3.2., p. 30).[1d] It was, thus, an obvious task to also try such protocols for some of the bipyridine building blocks available in our laboratory. Two different bipyridine containing acetylenes, **100b** and **105**, were sought in order to prepare macrocycle **106** (Scheme 49). From the first one the macrocycle could form by an intermolerular reaction between two **100b**, followed by an intramolecular reaction of the resulting compound (a). Initial results on this procedure were already available by Henze.[57] From the second one, which is a non-symmetrical building block and a direct cycle-precursor, **106** could form by an intramolecular reaction (b).

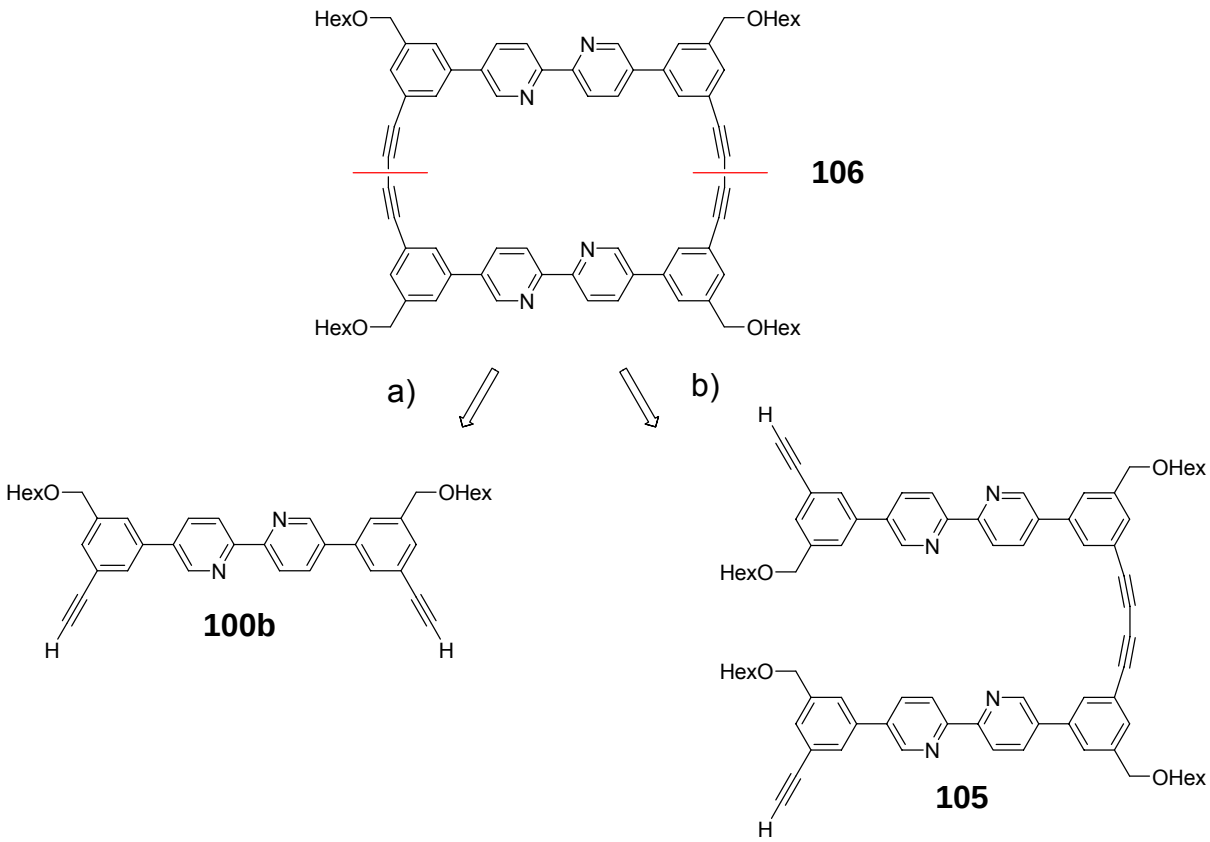

Scheme 49. Retrosynthetic strategies for the synthesis of bipyridine containing macrocycle **106**: from **100b** (a) and from **105** (b).

Synthesis of macrocycle 106 by an oxidative coupling of 100b

The synthetic sequence is outlined in scheme 50. It starts with a Sonogashira reaction of **76** with TMSA followed by the TMS group cleavage in basic conditions to furnish **100b** as described before (Chapter 4.2.).

The cyclization of **100b** was done using both Glaser and an Eglinton/Galbraith acetylene-acetylene coupling conditions.[71] For these reactions a large amount of Cu^{+}/Cu^{2+} was used. In order to decomplex the Cu ions from bipyridines after cyclization, a solution of KCN in water had to be used. This caused formation of an emulsion which complicated the work-up considerably and led to a loss of more than half of the material. This loss of substance could fortunately be overcome by treating the raw solid product with an aqueous solution of KCN. The precipitate, representing a mixture of oligomers, was then filtered and washed several times with water.

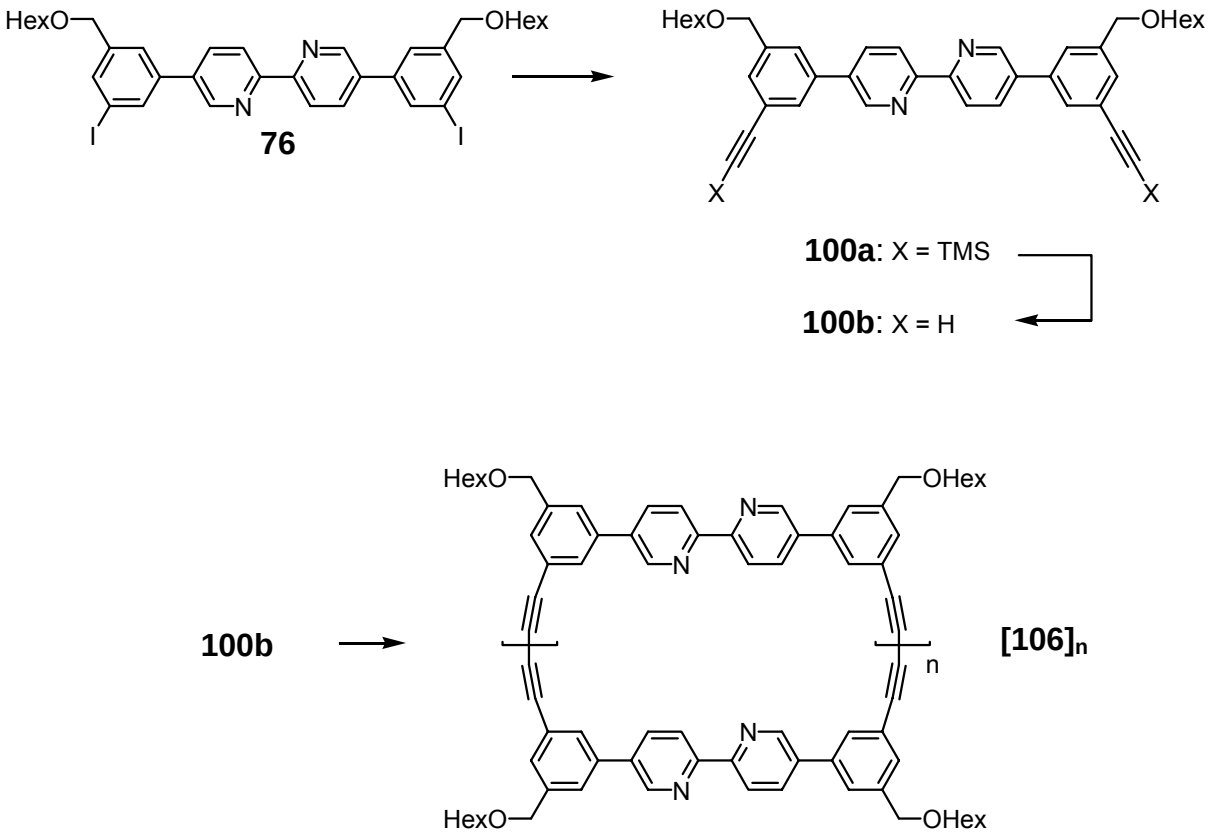

Scheme 50. Synthesis of ring precursor **100b** and its ring closure.

The raw product was analyzed by analytical GPC which showed three sharp peaks and a broad one (Figure 54Ad). The corresponding products were separated by preparative GPC but could unfortunately not be obtained in pure form directly. Therefore an additional purification step by column chromatography had to be done. The structures of the thus obtained compounds were established as **106** (cyclic dimer), $\mathbf{[106]_{1.5}}$ (cyclic trimer), and $\mathbf{[106]_2}$ (cyclic tetramer) on the basis of mass spectrometric and ^{1}H and ^{13}C NMR spectroscopic studies (Figure 54, 55, 56 and 57). Figure 54 contains an assignment of these compounds to their respective GPC peaks and also the corresponding MALDI-TOF mass spectra molecular ion peaks.

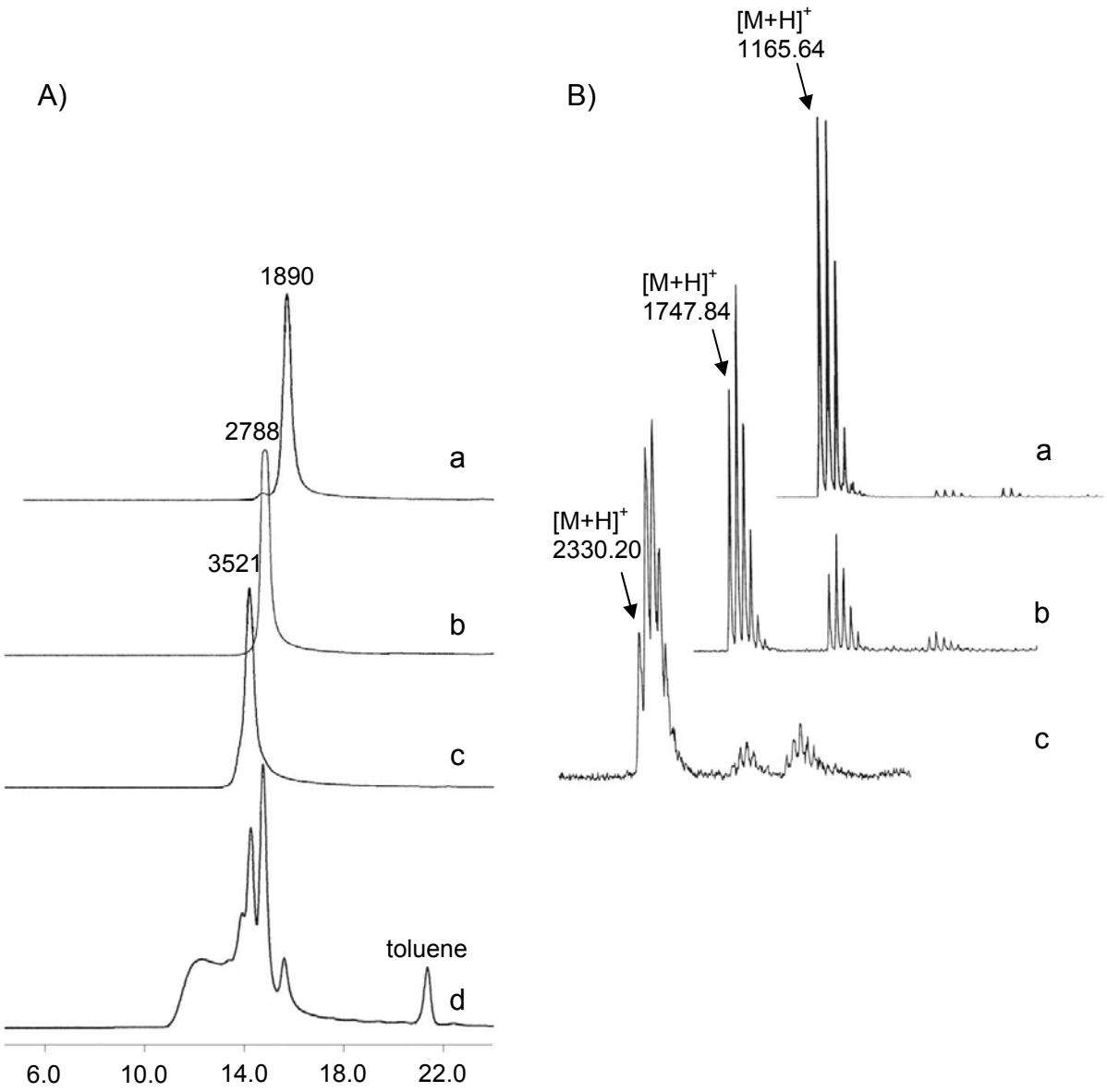

Figure 54. A) The GPC curves of **106** (Aa), **[106]$_{1.5}$** (Ab), **[106]$_2$** (Ac), and raw reaction mixture (Ad); B) MALDI-TOF mass spectra of macrocycles **106** (Ba), **[106]$_{1.5}$** (Bb), **[106]$_2$** in dithranol matrix (Bc). Only the enlarged parts of the isotopically resolved [M+H]+ signal are depicted.

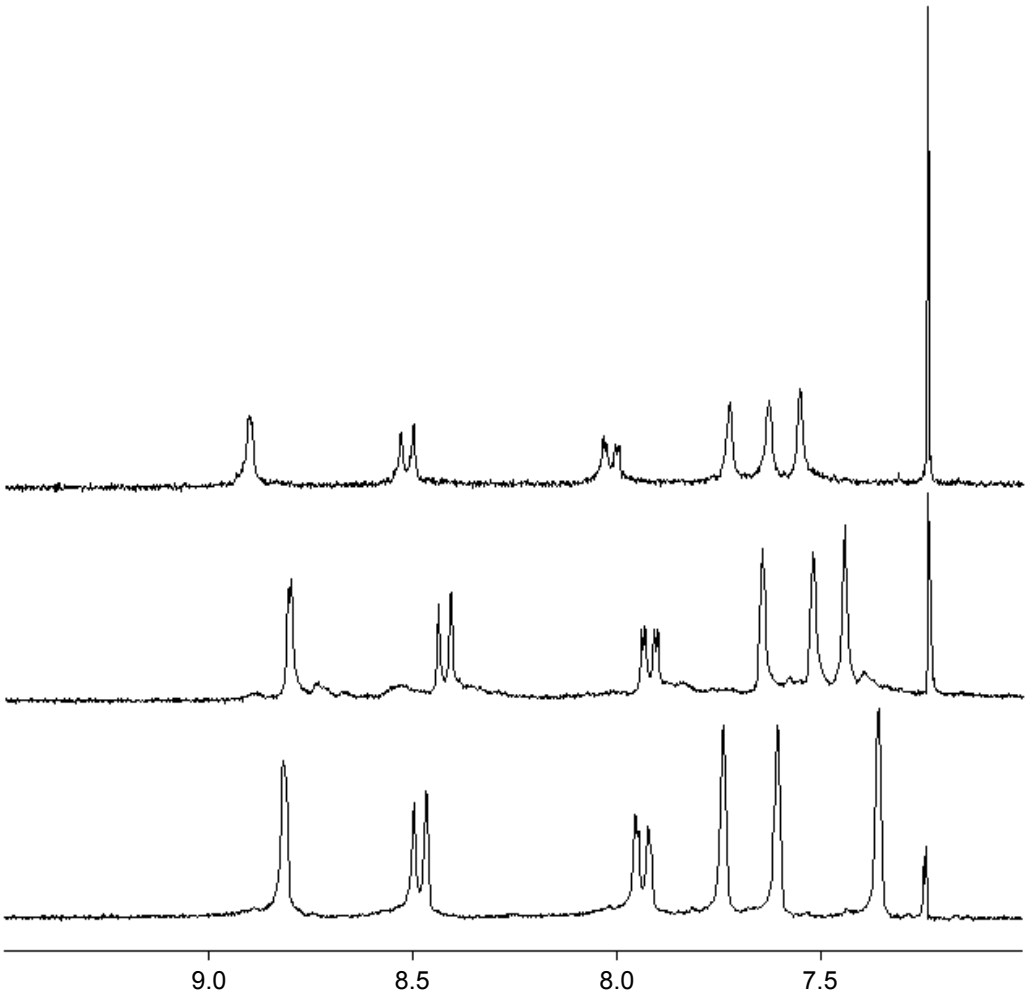

Figure 55. ^{1}H NMR spectra of **[106]$_2$** (a), **[106]$_{1.5}$** (b), and **106** (c) (*: $CDCl_3$, 270 MHz, 20 °C).

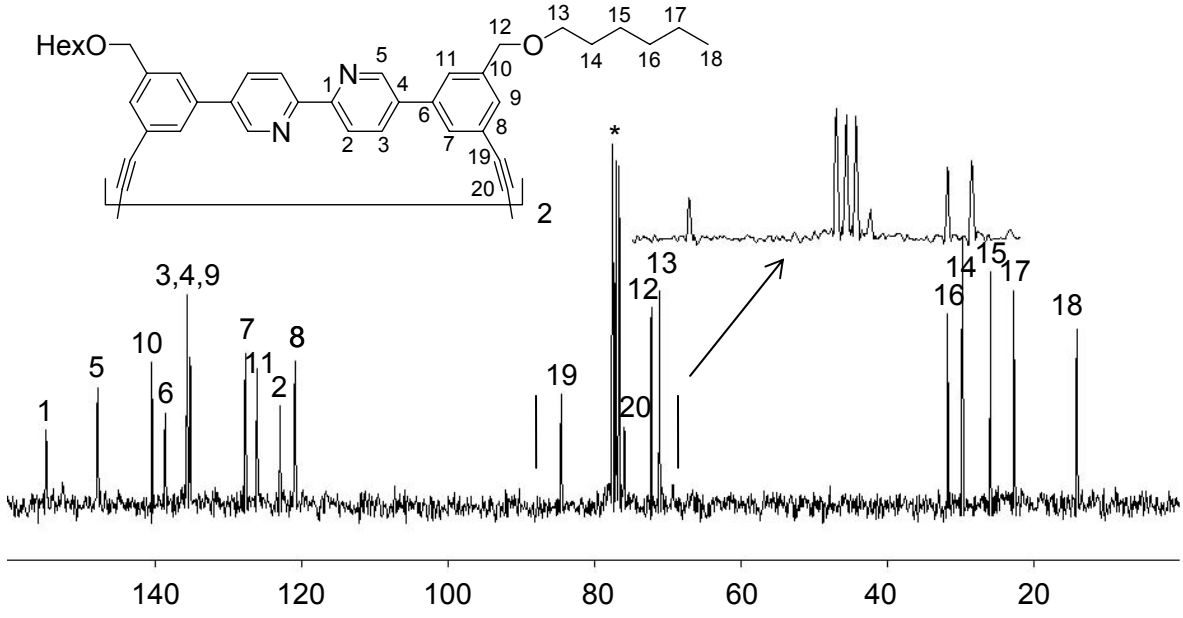

Figure 56. ^{13}C NMR spectrum of **106** (*: $CDCl_3$, 63 MHz, 20 °C).

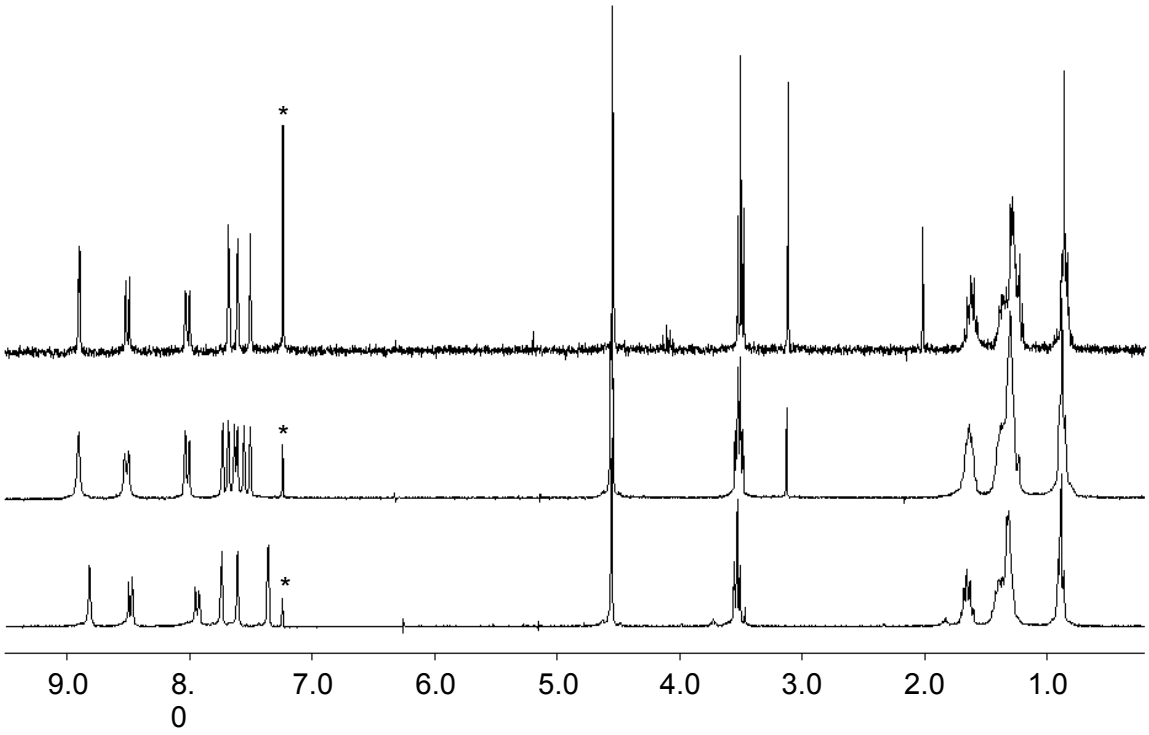

Figure 57. ^{1}H NMR spectra of **100b** (top), **105** (middle), and **106** (bottom) (*: $CDCl_3$, 270 MHz, 20 °C). The disappearance of the characteristic singlet signal at δ = 3.0 ppm of free acetylene protons of **100b** in the ^{1}H NMR spectrum of **106** is an additional prove for its cycle nature.

Macrocycle **[106]$_{1.5}$** contains three bipyridine units and has a hexagonal shape and has potential as building block for 2D network synthesis (Figure 58).

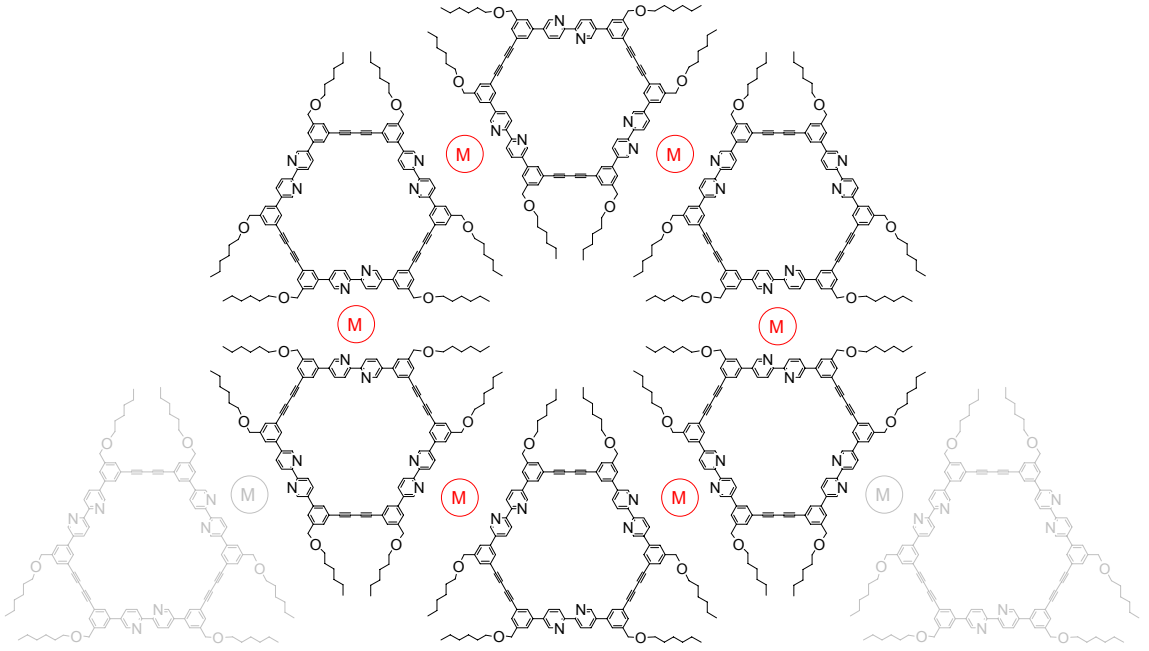

Figure 58. Imaginative 2D network using macrocycle **[106]$_{1.5}$** as building block.

Two structures can explain the double molecular mass of compound **[106]$_2$**. It can be either a larger macrocycle or consist in two intertwined macrocycles **[106]**, which would be a [2]catenane. It was difficult to differentiate between these two structure proposals by NMR or MS measurements. Unfortunately single crystals suitable for X-ray diffraction analysis could not be grown.

Synthesis of macrocycle 106 from cycle precursor 105

Macrocycle **106** was also prepared via route b) (Scheme 49). For this purpose a non-symmetrical building block **105** was required as mentioned above. An efficient synthesis to **105** was developed (Scheme 51). It contains conventional steps including Suzuki, Stille, and Sonogashira cross-coupling reaction. The synthesis of keystones **84**, **85**, and **86a**-**c** was described before in chapter 3.2.

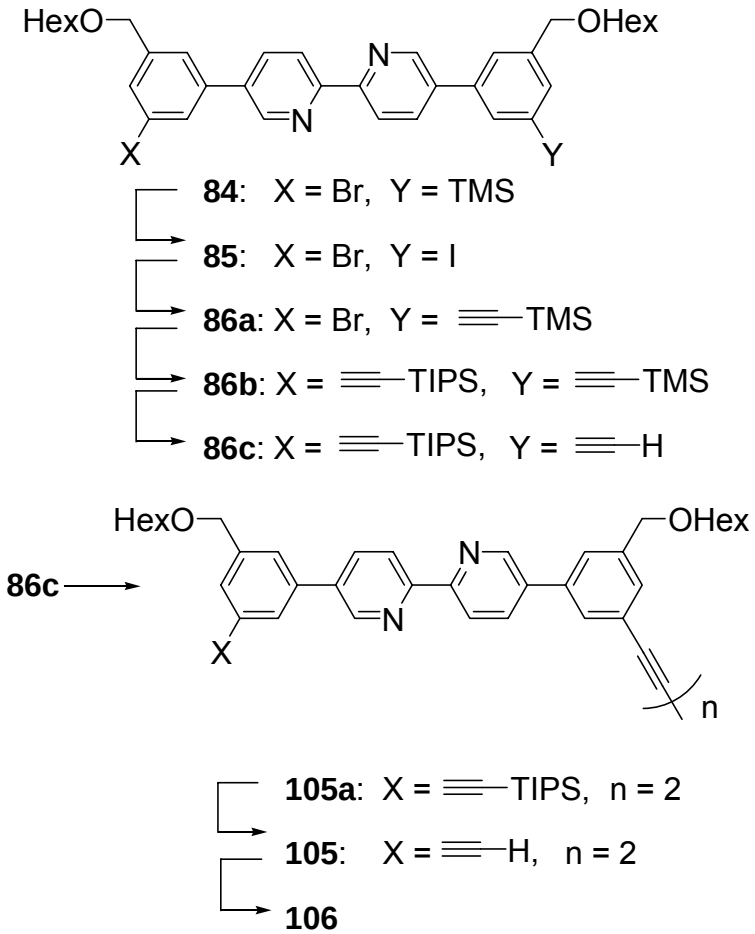

Scheme 51. Synthesis sequence to non-symmetrical building block **105** and its ring closure.

Pd^{2+} coupling of **86c** and subsequent deprotection of the resulting **105a** afforded the dimeric cycle precursor **105**. Its high purity can be easily assessed from its ^{1}H NMR spectrum (Figure 57, middle). Compound **105** was subjected to cyclization under air using $PdCl_2(PPh_3)_2$ and CuI in piperidine/THF at room temperature. The raw product analyzed by analytical GPC. The elution curve showed two sharp signals and a broader one. The first compound eluted at the same retention time like **[106]$_2$** and the second one at a retention time which was in between that of **[106]$_{1.5}$** and **[106]**. Since from this reaction, the trimeric cycle **[106]$_{1.5}$** cannot form and the ^{1}H NMR spectrum of the second compound differs from that of **[106]**, the only structures possible for this second compound are two intertwined macrocycles **[106]** or a complex of **106**. This matter is still under investigation.